Molecular Therapy
Oncology
Original Article

TYRP1 directed CAR T cells control tumor progression in preclinical melanoma models

Christopher S. Hackett,[1,2,3,10] Daniel Hirschhorn,[2,3,10] Meixian S. Tang,[2,3] Terence J. Purdon,[4] Yacine Marouf,[2,3] Alessandra Piersigilli,[5,9] Narasimhan P. Agaram,[6] Cailian Liu,[2,3] Sara E. Schad,[2,3] Elisa de Stanchina,[7] Sarwish Rafiq,[8] Sebastien Monette,[5] Jedd D. Wolchok,[1,2,3,10] Taha Merghoub,[2,3,10] and Renier J. Brentjens[4,10]

[1]Department of Medicine, Weill Cornell Medicine, New York, NY 10065, USA; [2]Swim Across America and Ludwig Collaborative Laboratory, Department of Pharmacology, Weill Cornell Medicine, New York, NY 10065, USA; [3]Parker Institute for Cancer Immunotherapy and Sandra and Edward Meyer Cancer Center at Weill Cornell Medicine, New York, NY 10065, USA; [4]Roswell Park Cancer Center, Buffalo, NY 14203, USA; [5]Laboratory of Comparative Pathology, Memorial Sloan Kettering Cancer Center, Weill Cornell Medicine, The Rockefeller University, New York, NY 10065, USA; [6]Department of Pathology, Memorial Sloan Kettering Cancer Center, New York, NY 10065, USA; [7]Human Oncology and Pathogenesis Program, Memorial Sloan Kettering Cancer Center, New York, NY 10065, USA; [8]Department of Hematology and Medical Oncology, Emory University School of Medicine, and Winship Cancer Institute, Atlanta, GA 30322, USA

Despite therapeutic efficacy observed with immune checkpoint blockade in advanced melanoma, many tumors do not respond to treatment, representing a need for new therapies. Here, we have generated chimeric antigen receptor (CAR) T cells targeting TYRP1, a melanoma differentiation antigen expressed on the surface of melanomas, including rare acral and uveal melanomas. TYRP1-targeted CAR T cells demonstrate antigen-specific activation and cytotoxic activity *in vitro* and *in vivo* against human melanomas independent of the MHC alleles and expression. In addition, the toxicity to pigmented normal tissues observed with T lymphocytes expressing TYRP1-targeted TCRs was not observed with TYRP1-targeted CAR T cells. Anti-TYRP1 CAR T cells provide a novel means to target advanced melanomas, serving as a platform for the development of similar novel therapeutic agents and as a tool to interrogate the immunobiology of melanomas.

INTRODUCTION

Therapeutic immune checkpoint blockade (ICB)[1] and tumor infiltrating lymphocytes (TILs)[2] have resulted in tremendous improvements in clinical outcomes in advanced melanoma and demonstrate the susceptibility of these tumors to T cell-mediated therapies. However, roughly half of patients ultimately progress on these therapies.[1,3] BRAF/MEK inhibitors are effective for the 50% of melanoma patients harboring BRAF mutations[4] and promising results have been observed with bispecific antibodies in uveal melanoma.[5] However, treatment options for ICB-refractory tumors (including tumors with low mutation burden), BRAF wild-type (WT) tumors, BRAF-mutant tumors that have developed resistance to BRAF/MEK blockade, and uveal, acral, and mucosal melanomas remain limited. These cases result in over 7,000 deaths annually in the United States[6] and represent an urgent unmet medical need for new therapies. Given the overall susceptibility of melanomas to immune-mediated therapies, alternative means of targeting T cells to tumor cells outside of classical T cell receptor (TCR)-mediated antigen recognition are of great interest. One mechanism by which melanomas evade T cells is through down-regulation of components of the antigen-presenting machinery required for tumor cell recognition by T cells and T cell activation.[7,8] Chimeric antigen receptors (CARs) are synthetic receptors containing an extracellular antigen recognition domain fused to a linker, transmembrane domain, and intracellular T cell activation and costimulatory domains.[9] These CARs give the T cells the ability to identify and eliminate tumor cells expressing surface antigens recognized by the CAR. Importantly, CARs target cell-surface molecules directly, rather than relying on antigen presentation by tumor cell antigen-presenting major histocompatibility (MHC) machinery, thus overcoming one mechanism of immune evasion by tumors.[10] Additionally, CARs can be designed to target endogenous antigens on tumor cells. This aspect overcomes some limitations of endogenous T cells, including TCR immune tolerance of naturally occurring antigens and the necessity for recognition of novel neo-antigens on tumors. These characteristics provide a potential means to target tumors that do not respond to current therapies in an HLA-independent manner.

The melanoma differentiation antigen tyrosinase-related protein 1 (TYRP1, gp75) is expressed on many melanomas, with expression

Received 5 April 2024; accepted 19 August 2024;
https://doi.org/10.1016/j.omton.2024.200862.

[9]Present address: Drug Safety Research and Evaluation, Takeda Development Center Americas, Cambridge, MA 02139, USA

[10]These authors contributed equally

Correspondence: Jedd D. Wolchok, Department of Medicine, Swim Across America and Ludwig Collaborative Laboratory, Parker Institute for Cancer Immunotherapy and Sandra and Edward Meyer Cancer Center at Weill Cornell Medicine, New York, NY 10065, USA.
E-mail: jdw2002@med.cornell.edu
Correspondence: Taha Merghoub, Swim Across America and Ludwig Collaborative Laboratory, Department of Pharmacology, Parker Institute for Cancer Immunotherapy and Sandra and Edward Meyer Cancer Center at Weill Cornell Medicine, New York, NY 10065, USA.
E-mail: tmerghoub@med.cornell.edu
Correspondence: Renier J. Brentjens, Roswell Park Cancer Center, Buffalo, NY 14203, USA.
E-mail: renier.brentjens@roswellpark.org

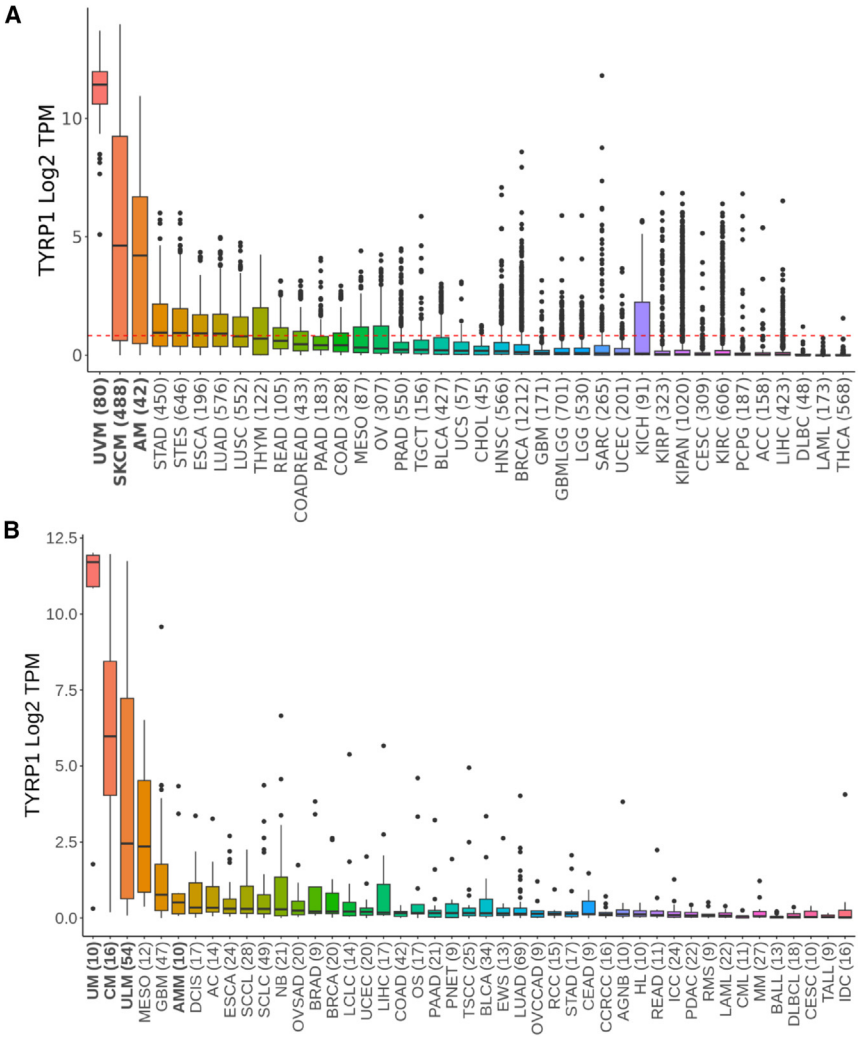

Figure 1. Analysis of TYRP1 mRNA expression in tumors

(A) TYRP1 RNA-seq expression in 17 TCGA cohorts (n = 13,325 samples) and Zhang C. et al. data (n = 57 samples), grouped by cancer type, sorted by median expression. Bolded groups represent melanoma subtypes. The dashed red line depicts the mean expression in the TCGA cohort. Abbreviations are explained in Table S1. (B) TYRP1 log2 TPM RNA-seq expression in the CCLE, grouped by cell line disease and sorted by median expression. Bolded groups represent melanoma subtypes. Abbreviations are explained in Table S2.

in normal tissues limited to melanocytes and other pigmented tissues.[11–13] Both human TYRP1 and mouse TRP-1 are recognized by the mouse monoclonal antibody TA99.[11–14] Of note, the monoclonal antibody IMC-20D7S, which binds the same TYRP1 epitope as TA99, demonstrated limited clinical efficacy with no dose-limiting toxicities in a Phase I clinical trial in melanoma patients,[15] suggesting TYRP1 is a valid and potentially safe target for melanoma therapy. TA99-based CAR T cells have been tested in syngeneic murine models,[16–19] and IMC-20D7S was recently demonstrated by another group as a valid binder to direct CAR T cells to melanomas in preclinical systems.[20] Here, we have used the antigen recognition domains of the TA99 antibody to generate a CAR targeting human melanoma cells. Human T cells transduced with this TYRP1-targeted CAR construct recognize and kill TYRP1$^+$ melanoma cells *in vivo*. Importantly, in contrast to TYRP1 TCR T cells, which showed profound T cell-mediated damage to pigmented tissues in the retina and uvea in mice,[21] the TA99-CAR showed minimal toxicity to normal tissues. While we did not observe frank tissue damage or inflammation in normal tissues, we did observe a loss of TYRP1$^+$ cells in some tissues, notably the uvea/choroid. These CAR T cells present a novel means to target immune-therapy refractory melanomas through an approach that overcomes limitations of TCR-dependent immune therapies and establish a platform to develop advanced CAR designs for solid tumors.

RESULTS

TYRP1 is expressed in melanomas

To confirm that TYRP1 is a suitable target for CAR T cells in melanoma, we assessed expression of *TYRP1* mRNA in the Cancer Genome Atlas (TCGA)[22] and the Acral and Cutaneous Melanoma Focused Dataset (ACMFD).[23] We noted particularly high expression in uveal, cutaneous, and acral melanoma; expression in uveal was considerably higher than the other two types (Figure 1A; the full names of the abbreviated TCGA cancer types are listed in Table S1). A separate analysis based on a query of the Cancer Cell Line Encyclopedia (CCLE)[24] again showed increased expression of TYRP1 in multiple melanoma subtypes, with relatively higher expression of TYRP1 in cell lines derived from uveal (UM), cutaneous (CM), and some other unannotated subtypes (ULM) of melanoma tumors, and to a much lesser extent in amelanotic melanoma (AMM) (Figure 1B; the full names of the abbreviated CCLE cancer types are listed in Table S2). We next assessed TYRP1 surface expression on several human and mouse melanoma cell lines demonstrating detectable TYRP1 on a subset of melanoma cell lines (Figure S1). To assess TYRP1 expression in normal tissue, we next examined the genotype-tissue expression (GTEx) project data, a database of gene expression in normal tissue.[25] We noted relatively higher expression in skin, heart, kidney, and lung tissues compared with the other normal tissues (Figure 2A). Early work on TYRP1 noted that the protein was only expressed in a subset of melanomas.[12,13] In order to differentiate TYRP1 high vs. low tumor samples based on RNA expression, we next plotted the distribution of TYRP1 mRNA expression levels of melanomas in TCGA and ACMFD datasets, noting a bimodal distribution (Figure 2B). To illustrate the difference in mRNA expression between

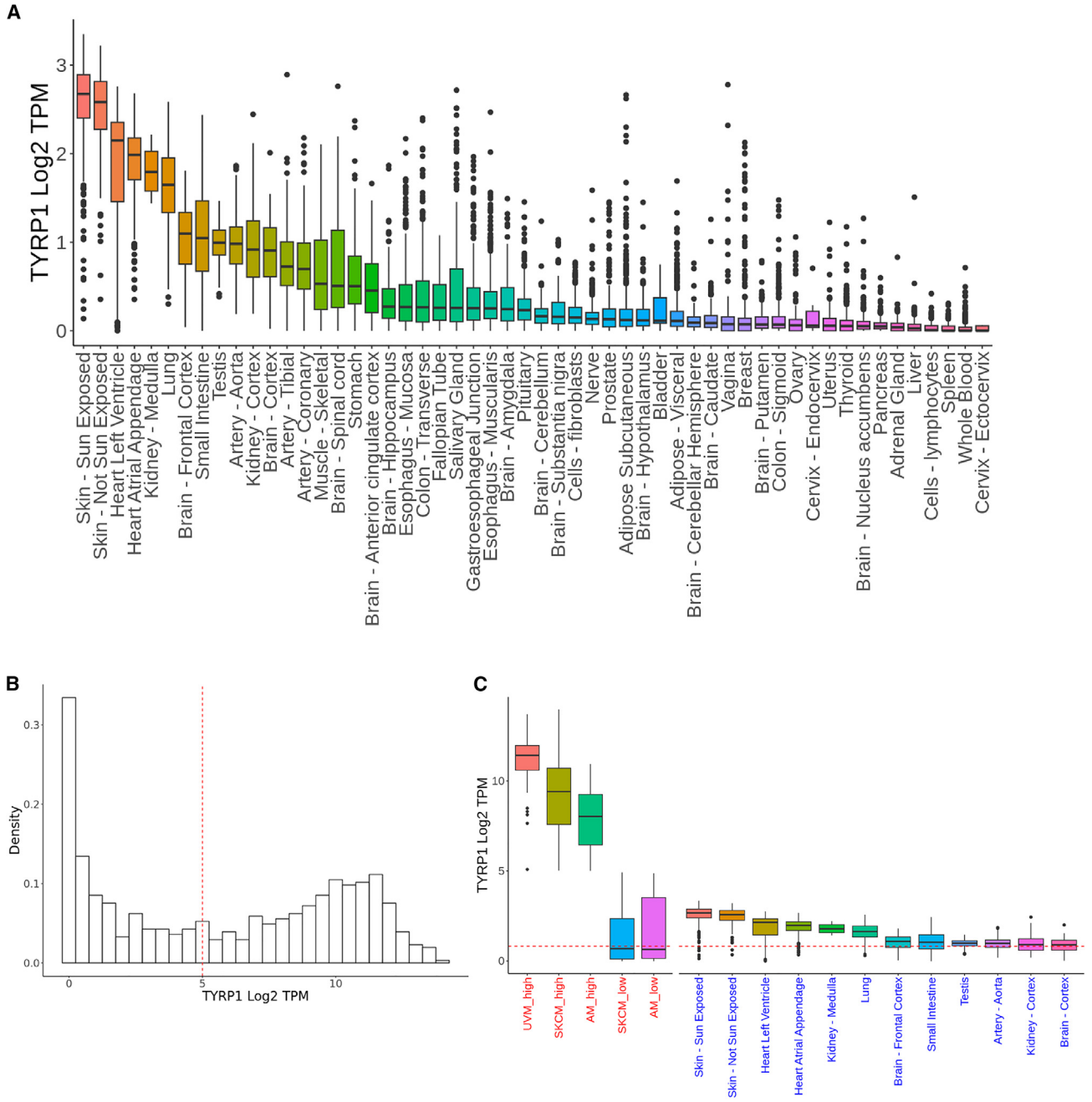

Figure 2. Analysis of TYRP1 mRNA expression in normal tissues and in comparison with melanomas

(A) TYRP1 expression in GTEx is shown grouped by detailed tissue type (SMTSD). Expression was measured by RNA-seq and $\log_2$ and TPM normalized. The tissue groups are ordered by median expression. (B) The density of TYRP1 RNA-seq expression in melanomas in the TCGA and Zhang et al. ACMFD tumor tissues ($\log_2$ TPM normalized). The dashed red line depicts the threshold used to separate samples into high and low expressers of TYRP1. (C) TYRP1 RNA-seq expression ($\log_2$ TPM normalized) was compared between melanoma tumor tissues and normal tissues. Three melanoma cohorts from TCGA and Zhang C. et al. were divided into high and low TYRP1 expression using $\log_2$ TPM of 5 (left, in red), and plotted with the 12 top TYRP1-expressing normal tissues grouped by detailed tissue type (SMTSD) from GTEx (right, in blue), sorted by median expression. The dashed red line depicts the mean expression of TYRP1 in all TCGA cohorts.

TYRP1-high melanomas (which may be candidates for targeted therapy) vs. normal tissues, we next split the melanomas into high vs. low expressors using $\log_2$ TPM of 5 as a cutoff, and plotted these groups vs. normal tissues with above-average mRNA expression compared with the average of all normal tissues, noting a substantial gap in expression between TYRP1-high melanomas and normal tissues

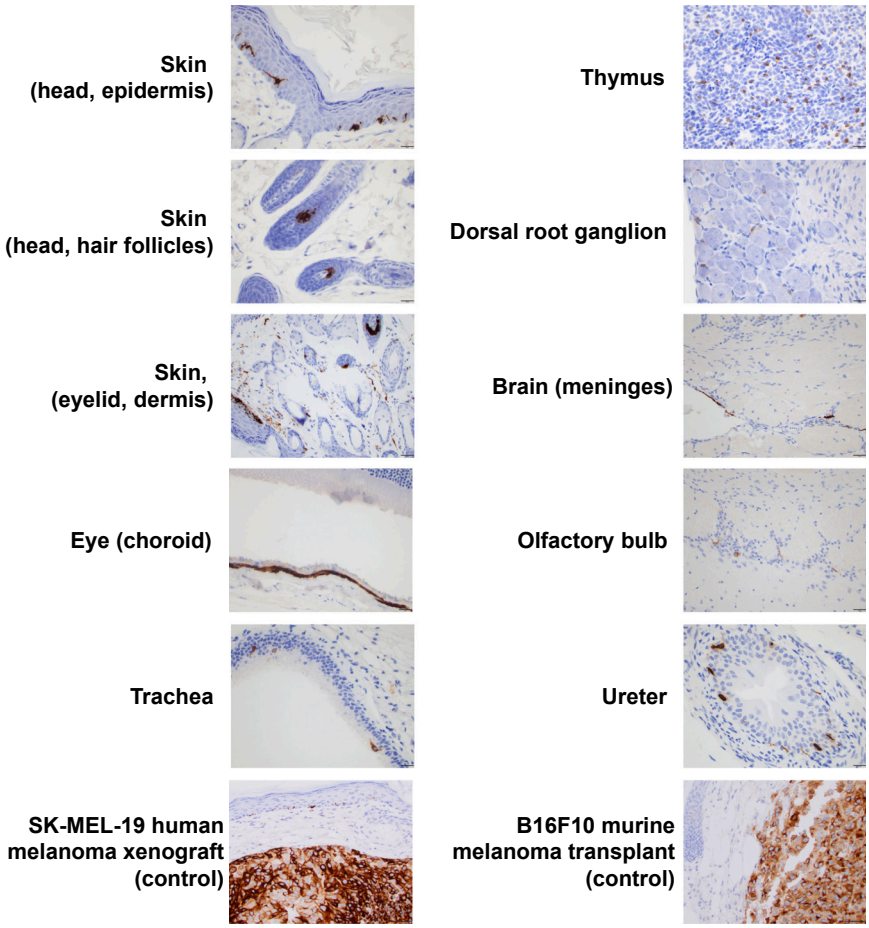

Figure 3. IHC for TYRP1 on mouse normal tissues
Representative tissues from whole-mouse necropsy were stained for TYRP1. Representative images from positive tissues are shown. Cells staining brown are immunoreactive against the anti-TYRP1 antibody EPR13063. Cells were additionally stained with hematoxylin. Scale bars represent 20 μm.

(Figure 2C). To further characterize tissue expression of TYRP1 in mice and assess changes mediated by TYRP1-targeted CAR T cells, we next stained normal tissues in tumor-bearing mice treated with off-target (MUC16) CAR T cells[26] for TYRP1 using immunohistochemistry (IHC). We noted immunoreactivity in skin, eyes (choroid/uvea), trachea, thymus, dorsal root ganglion, meninges, olfactory bulb, and ureter (Figure 3), but in no other normal tissues. Of note, we did not detect protein immunoreactivity in heart or kidney despite RNA expression noted in the GTEx database.

Human TA99-CAR T cells demonstrate antigen-specific cytotoxicity and cytokine release *in vitro*

To construct a human TYRP1-targeted CAR, we used the heavy and light chain variable regions of the TA99 antibody[12,13] to generate an FLAG-tagged scFv, then fused this to a portion of CD28 containing the extracellular juxta membrane, transmembrane, and intracellular portions, followed by the CD3ζ chain (Figure 4A). We used a GalV9 SFG gamma retroviral vector to introduce this construct into primary human T cells, routinely achieving transduction efficiencies of 60% to over 90% (representative profile shown in Figure S2A). We next validated that negative control cell lines Nalm6 did not express TYRP1 (Figure S2B), and that the human melanoma cell lines did not express CD19 (a protein expressed on B cells and targeted by the CD19-CAR[27]) (Figure S2C) or MUC16 (an ovarian tumor antigen targeted by the 4H11 CAR[26]) (Figure S2D). We next transduced TYRP1$^-$ Chinese hamster ovary (CHO) cells with a truncated, surface localized human TYRP1 (Figure S2E). To assess antigen-specific tumor killing activity of human TA99-CAR T cells *in vitro*, we co-cultured TA99-CAR T cells with TYRP1$^+$ SK-MEL-19 and SK-MEL-188 human melanoma cells at different ratios. We observed significant killing of melanoma cells by TA99-CAR T cells compared with CD19-targeted (CD19-28z)[27] CAR T cell and MUC16-targeted (4H11-28z)[26] CAR T cell negative controls (Figures 4B, S3A, and S3B). In addition, at effector to tumor cell ratios below 1, TA99-CAR T cells were unable to kill TYRP1$^-$ CD19$^+$ NALM-6 leukemia cells targeted by the CD19-CAR or the TYRP1-low melanoma cell line SK-MEL-28 (Figures 4C, S3C, and S3D). To assess antigen-specific T cell activation, we next co-cultured TA99-CAR T cells with either WT or TYRP1(truncated) CHO cells. In comparison with TA99-CAR T cells alone or TA99-CAR T cells co-cultured with TYRP1$^-$ WT CHO cells, TA99-CAR T cells co-cultured with TYRP1(truncated)$^+$ CHO cells released cytokines granulocyte-macrophage colony-stimulating factor (GM-CSF), interferon (IFN) γ, interleukin (IL)-2, and tumor necrosis factor (TNF)α, indicating antigen-specific T cell activation (Figure 4D). Similarly, TA99-CAR T cells demonstrated higher levels of cytokine release when co-cultured with TYRP1$^+$ SK-MEL-19 human melanoma cells compared with B cell-targeted CD19-CAR T cells and ovarian cancer-targeted 4H11-CAR T cells (Figure 4E). Altogether, these observations suggested that TA99-CAR T cells are functional and show specific cytolytic activity against TYRP1-expressing human melanoma cells.

Human TA99-CAR T cells demonstrate anti-melanoma efficacy *in vivo*

To further assess the efficacy of TA99-CAR T cells against TYRP1$^+$ human melanomas, we next established an *in vivo* xenograft model. Two million SK-MEL-19 human melanoma cells transduced with a retrovirus encoding a green fluorescent protein-firefly luciferase fusion protein (GFPffLuc) construct were implanted subcutaneously

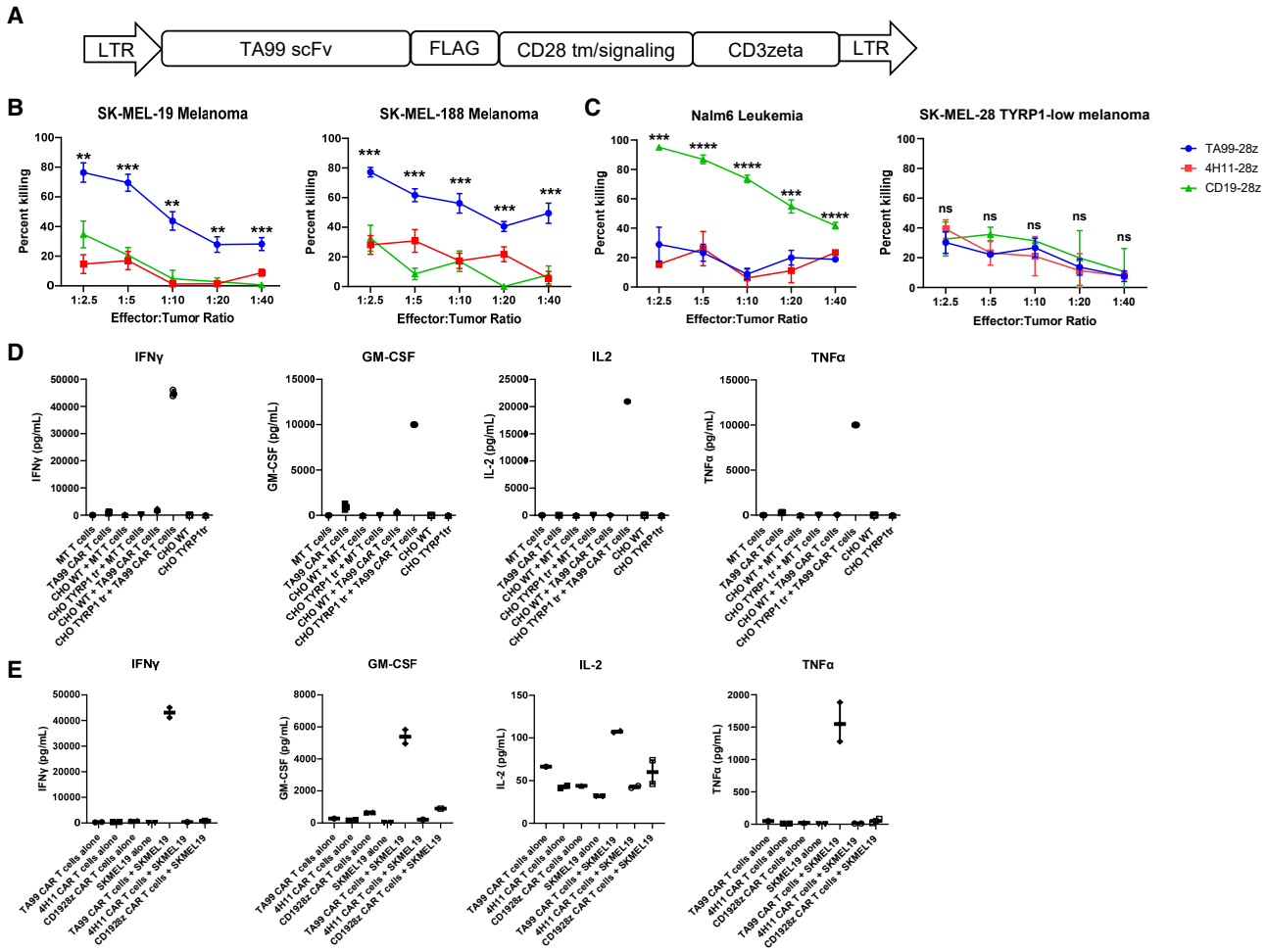

Figure 4. Human TA99-CAR T cells have efficacy against human melanomas *in vitro*

(A) Schematic of TA99-CAR harboring a TYRP1 scFv binder based on the murine anti-TYRP1 TA99 antibody, CD28 transmembrane and costimulatory domain, and CD3zeta activation domain in an SFG gamma retroviral vector. (B) Human CAR T cells were co-cultured with TYRP1$^+$ SK-MEL-19 and SK-MEL-188 melanoma cells expressing firefly luciferase at varying effector:T cell ratios and cytotoxicity was assessed using bioluminescence after 24 h. TA99-CAR T cells demonstrated superior antitumor efficacy compared with ovarian-targeted 4H11-CAR and anti-CD19 CAR T cells. (C) Human CAR T cells were co-cultured with CD19$^+$, TYRP1$^-$ Nalm6 leukemia cells and TYRP1^{low} SK-MEL-28 human melanoma cells. TA99-CAR T cells showed minimal cytotoxicity compared with the CD1-CAR controls in Nalm6 cells, and no CAR T cells demonstrated cytotoxicity against the SK-MEL-28. For (B) and (C), $^*p < 0.05$, $^{**}p < 0.005$, $^{***}p < 0.0005$, $^{****}p < 0.00005$ by unpaired t test adjusted for multiple comparisons. NS = not significant. Means (SDs) are plotted. (D) Cytokine levels of TA99-CAR T cells cultured alone or with various CHO cell lines, demonstrating that CAR T cells only released cytokines in response to CHO cells expressing TYRP1. MT = mock transduced, TYRP1 tr = exogenous expression of truncated (membrane localized) TYRP1. (E) Cytokine levels of various CAR T cells co-cultured with TYRP1$^+$ SK-MEL-19 melanoma cells, demonstrating that TA99-CAR T cells showed increased cytokine release compared with CAR T cells targeted to non-melanoma antigens.

into the flanks of NSG mice and allowed to establish tumor masses for 10 days. We then administered 5 million or 0.5 million CAR T cells intravenously via tail vein injection (Figure 5A). Tumor volume was assessed weekly using caliper measurements (Figures 5B, S4A, and S4B) and *in vivo* imaging of firefly luciferase bioluminescence (Figures 5C, S4C, and S4D). We observed a significant reduction in tumor volume in mice that received TA99-CAR T cells compared with negative control mice that received a CAR targeting MUC16 (4H11),[26] an ovarian cancer antigen not expressed on SK-MEL-19 cells, or CD19, present on B cell leukemias and lymphomas but not on melanomas, and compared with mice that received no T cells. As expected, all mice that had received a dose of 5 million human T cells developed clinical signs of xenogeneic graft vs. host disease (xGvHD; usually presenting with lethargy and unkempt coat) by 2 months of age and were euthanized. Although tumors in the TA99-CAR T cell-treated group were considerably smaller than those in the control groups, the remaining tumor mass contained viable tumor cells. Staining for TYRP1 in the residual TA99-CAR T cell-treated tumors demonstrated strong expression of TYRP1 (Figure 5D), suggesting that antigen escape was not the mechanism of

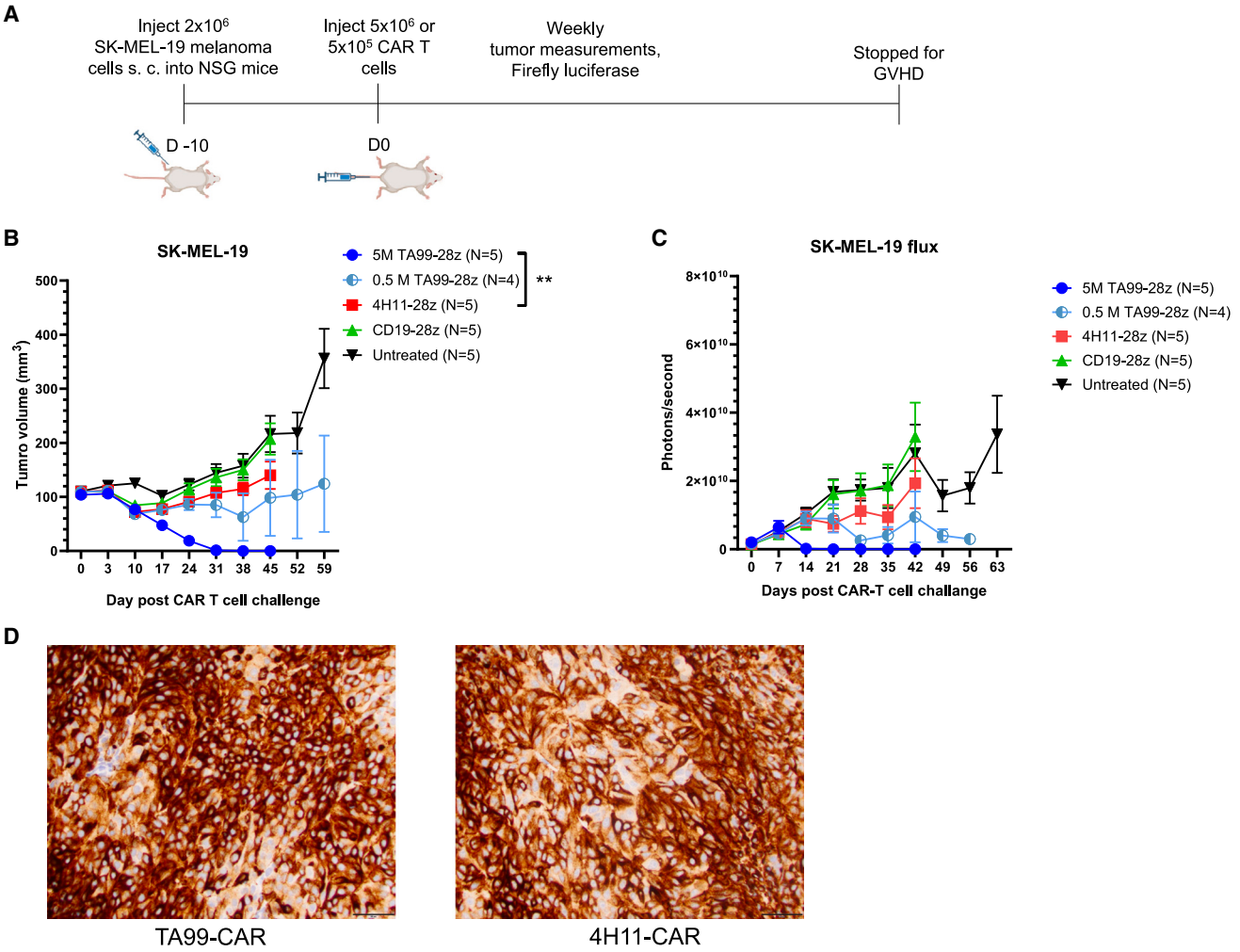

Figure 5. TA99-CAR T cells have efficacy against human melanomas *in vivo*

(A) Schematic of *in vivo* experiments. Two million SK-MEL-19 melanoma cells were injected subcutaneously. After 10 days of engraftment, CAR T cells were injected (5 million, with the exception of 0.5 million for one cohort of TA99-CAR T cells). Tumor growth was assessed weekly using bioluminescence and caliper measurements. Image created with the assistance of BioRender.com. (B) Tumor growth of mice treated with various CAR T cells (note that one mouse in the 0.5M TA99 CAR T cell cohort died of unknown causes during week 2 and was excluded from analysis). $^{**}p = 0.000561$ at day 45 by unpaired t test. All mice who received human CAR T cells developed xenogeneic graft vs. host disease (xGvHD); mice were euthanized when clinically indicated per our IACUC protocol and analysis of the cohort was stopped when the first mouse developed xGvHD. (C) Quantitation of the bioluminescence signal from mice in (B). (D) TYRP1 was assessed by IHC in residual tumor tissue from the mice treated in Figures S4B and S4C. Scale bars represent 50 μm. For (B) and (C), means (SEMs) are plotted.

incomplete tumor clearance. These observations suggested that, while TA99-CAR T cells are capable of human melanoma control, they do not achieve complete eradication of TYRP1^{+} tumor cells.

TA99-CAR T cells cause minimal toxicity to normal tissue

A primary concern with CAR T cell therapy is toxicity to normal tissue due to the CAR T cells recognizing antigen expressed in non-malignant cells ("on-target, off-tumor" toxicity). To further assess for potential CAR T cell toxicity to normal tissues, we performed full pathological analysis on mice treated with human TA99-CAR T cells, using mice treated with human 4H11-CAR T cells as the negative control, once mice reached a clinical toxicity endpoint driven by xGvHD during week 5 post T cell infusion. Postmortem histological analysis of normal tissues in a subset of mice revealed that all mice that had received human T cells developed minimal to mild lymphocyte infiltrate with morphological features consistent with xGvHD in several organs, including skin and liver. This pattern was observed in multiple animals from both the TA99-CAR and 4H11-CAR treatment cohorts (Figure S5).

The antibody TA99 recognizes both human and mouse TYRP1,[11,14] suggesting that TA99-CAR T cells may recognize TYRP1 on normal mouse tissues in a way that might predict antigen-specific clinical toxicity in humans. TYRP1 is expressed on normal

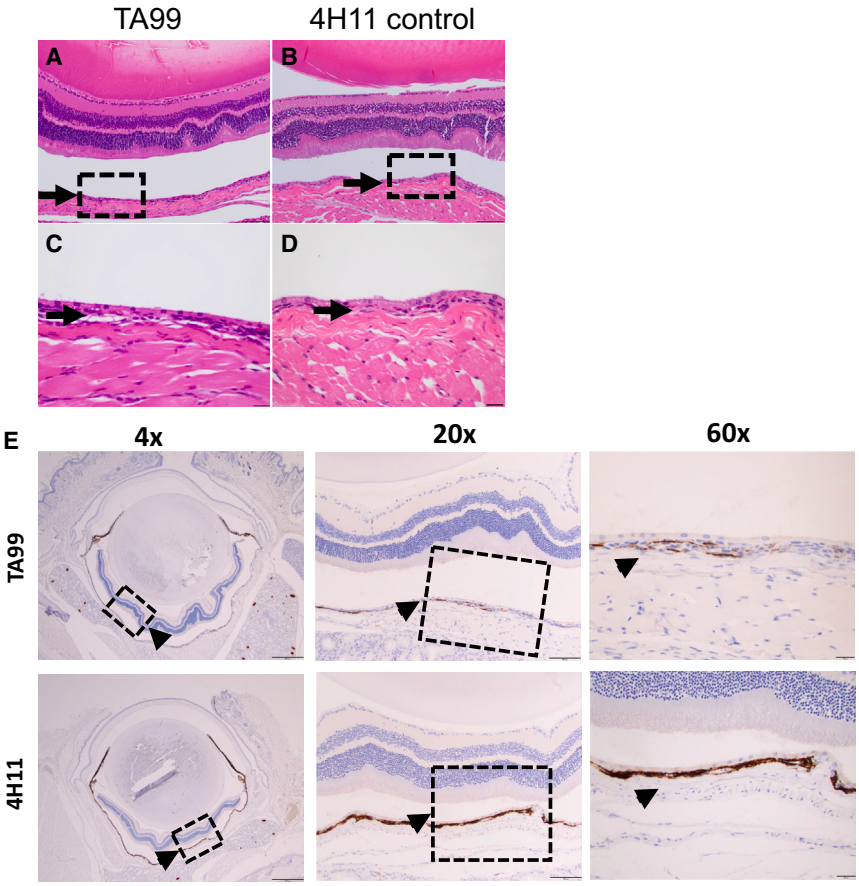

Figure 6. Histological analysis of eye tissue from CAR T cell-treated mice

(A–D) Hematoxylin-eosin staining of cross sections of eyes from mice treated with either TA99-CAR T cells (A and C) or off-target 4H11-CAR T cells (B and D) (from Figure S4B) at various magnifications. Note that retinal separation was an artifact of tissue fixation. Scale bars represent 100 μm (A and B) or 20 μm (C and D). (E) IHC for TYRP1 on cross sections from mice treated with TA99-CAR T cells or off-target 4H11-CAR T cells, showing a loss of TYRP1$^+$ cells in the uvea/choroid of mice treated with the TA99 CAR relative to the 4H11 controls. Scale bars represent 500 μm (left), 100 μm (center), and 20 μm (right).

melanin-producing cells[11–14] including the skin and the pigmented choroid, and prior investigations targeting TYRP1 using a TCR resulted in profound ocular toxicity.[21] We investigated the uvea of mice treated with both TA99-CAR and 4H11-CAR and found no lymphocytic infiltrate into uveal or retinal tissues in either group (Figures 6A–6D). In contrast to experiments using a TYRP1-targeted TCR,[21] we did not see inflammation, edema, or other evidence of immune-mediated damage to eye tissue by standard histology (Figures 6A–6D). However, we did note partial loss of TYRP1$^+$ cells in the posterior choroid by IHC for TYRP1 in five of five mice in the treated cohort, although the anterior eye demonstrated comparable staining for TYRP1 (Figures 6E and S6).

We next compared other TYRP1$^+$ normal tissues in control mice compared with mice that had received the TA99-CAR T cells. We also noted loss of TYRP1$^+$ cells in the skin, meninges, and thymus, although these tissues did not demonstrate other evidence of inflammation or immune infiltration (Figure 7). Interestingly, we did not see loss of TYRP1$^+$ cells in the hair follicle, olfactory bulb, or dorsal root ganglia of mice treated with TA99-CAR T cells (Figure S7). The lack of inflammation and minimal tissue toxicity observed after infusion of human TA99-CAR T cells suggests that TYRP1 is a suitable target for CAR T cell therapy against melanoma, though the loss of TYRP$^+$ cells in some tissues, particularly in the eye, warrants further investigation.

DISCUSSION

Immune checkpoint blockade and tumor infiltrating lymphocyte therapies have resulted in improvements in advanced melanomas, demonstrating an increased sensitivity to T cell-mediated therapies compared with other solid tumors.[2,28,29] Nevertheless, many melanomas do not respond to or develop resistance to these therapies,[30] likely for numerous reasons that are not fully characterized, necessitating alternative treatment approaches. CAR T cells targeted to melanomas could complement these therapies by providing an opportunity to target T cells to melanomas using melanoma-specific surface antigens rather than MHC-presented antigens. CAR T cells may recognize antigens overexpressed on the surface of tumor cells in a way that endogenous TCRs, which have undergone selection for tolerance of native antigens and depend on the MHC antigen-presentation machinery, cannot.[10] In this way, optimized CAR T cells have the potential to be effective against melanomas that do not respond to current immune and cellular therapies, particularly melanomas with low mutational burden (and thus few unique tumor associated antigens), including uveal, acral, and mucosal melanomas, as well as those with a disruption in antigen-presentation machinery.

We have generated CAR T cells targeting TYRP1 on melanomas using the antigen recognition regions of the well-characterized antibody TA99. TA99-CAR T cells demonstrate antigen-specific antitumor activity *in vitro* and *in vivo*. This novel CAR may serve as both a basis for potential therapy for advanced melanomas, as well as a platform to test and optimize further CAR modifications and combination therapies.

Antigen-dependent toxicity to normal tissues is a primary concern for targeted cellular therapies and has been observed in clinical trials of CAR T cells.[31,32] As TYRP1 is expressed in pigmented melanin-producing tissues, there is a theoretical concern for

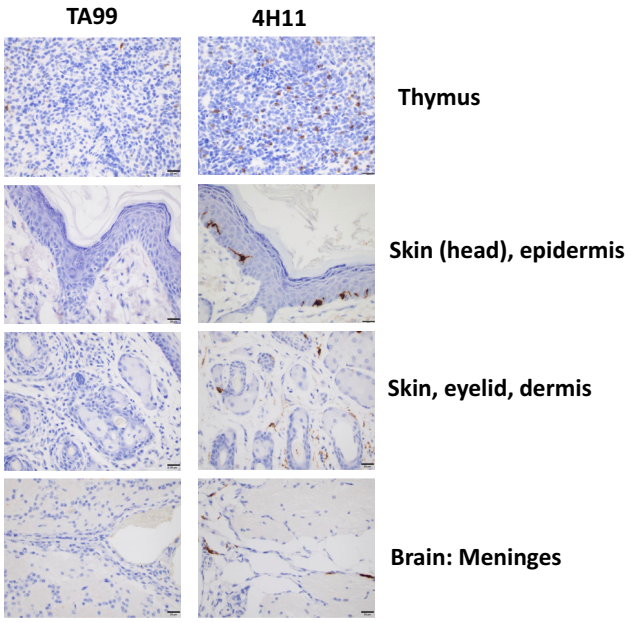

Figure 7. Loss of TYRP1+ cells in normal tissues of mic treated with TA99 CAR T cells

Tissues from mice from cohorts shown in Figure S4B were collected and stained for TYRP1 using IHC. We noted reduced levels of TYRP1$^+$ cells in thymus, skin, and meninges in mice that received TA99 CAR T cells. Note that the 4H11 cohort are from the same source as images from Figure 3, shown again for comparison. Scale bars represent 20 μm.

on-target, off-tumor toxicity to tissues such as skin, eye, and substantia nigra. Encouragingly, meaningful albeit transient clinical responses were observed without any dose-limiting or other concerning toxicities in a clinical trial of a human anti-TYRP1 antibody,[15] suggesting that targeting TYRP1 in melanomas is feasible. However, cellular therapies have the potential for more dangerous toxicities compared with antibody therapies. Concerningly, profound ocular and dermatologic toxicity was seen in a preclinical model of transgenic TYRP1-targeted TCRs.[21] While our group has also observed this ocular and dermatologic toxicity with the TYRP1 TCR (data not shown), we do not observe any equivalent toxicity using TA99-CAR constructs. This discrepancy may be due to multiple factors. Notably, TCRs recognize intracellular antigens presented on MHC/HLA molecules, while CARs recognize antigens expressed directly on the cell surface.[33] Most TYRP1 in normal tissues is confined to melanosomes within the cell, with only a small fraction on the cell surface,[34] which may be below the threshold necessary to activate a TYRP1-targeted CAR. However, melanosomal TYRP1 antigens may be presented on MHC/HLA molecules and "visible" to a T cell expressing a TYRP1-targeted TCR. In contrast to normal tissue, many melanomas express TYRP1 on the cell surface, which is accessible to a T cell expressing a CAR at a level sufficient to induce T cell activation. TCR may be more sensitive to low levels of TYRP1 by an additional mechanism. A single TCR may be activated by binding to a single antigen molecule, as antigen binding to the α and β chains alters the intracellular conformation of the receptor in a way that activates downstream signaling pathways. In contrast, CAR receptors may require over 100 antigen molecules for activation of intracellular signaling through aggregation of CAR molecules,[35] since antigen binding to the CAR alone does not induce a conformational change in the intracellular signaling domains in a way similar to the way antigen binding to the TCR components induces the assembly of the TCR intracellular signaling complex. Thus, the threshold for CAR activation may be much higher than an equivalent TCR even in cases where the CARs are based on antibodies with much higher antigen affinities than TCRs. Due to this, CAR T cells may require much higher levels of antigen expression on tumor cells for activation compared with TCRs,[36,37] providing a therapeutic window if antigen expression levels are higher on tumor than on normal tissues. Thus, CAR T cells may distinguish tumor cells from normal tissues in cases where the target antigen is expressed at high levels on the tumor cell surface but at relatively lower levels and with more intracellular localization in normal tissues. Interestingly, we did see reduction of TYRP1$^+$ cells in some tissues, though without other evidence of immune-mediated tissue destruction. Further and more thorough preclinical safety testing will be required prior to clinical trials of TYRP1-targeted CAR T cells against melanoma. Nevertheless, this system provides a platform for further development of "armored" CAR T cells that overcome inhibitory signals in solid tumors,[9] potentially introducing novel treatment options for melanomas and illuminating avenues to clinical efficacy for other solid tumors.

MATERIALS AND METHODS

Assessment of TYRP1 mRNA in tumors and normal tissues

The expression of TYRP1 was obtained from TCGA RNA-sequencing (RNA-seq) data[22] and compared among the 17 different cohorts (cancer types) with a total of 13,325 samples. Due to the lack of an acral melanoma cohort in TCGA, bulk RNA data from Zhang et al.[23] were obtained, which contained 57 samples (42 acral [AM], 15 cutaneous [SKCM]). The GTEx Bulk RNA-seq tissue expression[25] V8 release data were used. The expression of TYRP1 is shown based on detailed tissue type (SMTSD). Both TCGA and Zhang et al. RNA expression data were obtained as raw counts, TPM normalized,[38] and then $\log_2$ transformed with a pseudo count of 1. CCLE gene expression data were obtained in $\log_2$ TPM normalized format, therefore, no further normalization was applied. GTEx data were only $\log_2$ normalized as they were obtained in TPM format. The boxplots were generated using the ggplot2 R package[39] (v3.4.3).

Generation of TA99-CARs and control CARs

The heavy and light chain variable regions were sequenced from the TA99 hybridoma generated at MSK. A single-chain variable fragment (scFv) was created by fusing the heavy chain variable fragment, a $G4S_3$ linker, and the light chain variable fragment. The scFv sequence was modified to remove cryptic polyadenylation signals. To create a human CAR construct, the signal peptide from human CD8 was fused to the TA99 scFv, which was fused to an FLAG epitope tag,

the extracellular juxtamembrane, transmembrane, and intracellular signaling domains of human CD28, followed by the intracellular domain of the human CD3 zeta chain. All constructs were generated by inserting custom-synthesized DNA gblocks (IDT, Coralville, IA) using the NEBuilder HiFi DNA Assembly master mix protocol (Cat# E262, New England Biolabs, Ipswich, MA). These constructs were cloned into an SFG gamma retroviral vector as previously described.[40] The anti-CD19 SJ25C1 CAR[27] was re-cloned to harbor V5 and myc epitope tags between the scFv and the CD28 hinge/transmembrane domain. The anti-MUC16 4H11 CAR[26] was re-cloned to harbor V5 and HA tags between the scFv and the CD28 hinge/transmembrane domain.

Cell lines and reagents

All SK-MEL cell lines were acquired from the Wolchok/Merghoub lab or through the MSK Biorepository. Nalm6 cells were obtained from ATCC. SK-MEL and Nalm6 cell lines were cultured in RPMI supplemented with 10% FBS (Thermo Fisher, Waltham, MA) and penicillin-streptomycin (pen/strep) (Cat# 15140163, Thermo Fisher, Waltham, MA). CHO cells were obtained from the Merghoub/Wolchok lab stock and maintained in RPMI supplemented with 10% FBS, pen/strep, 2 mM L-glutamine, sodium pyruvate, and non-essential amino acids (MSK Media Core Facility). Cells were tested for mycoplasma and validated by STR testing through ATCC. Cell lines used in bioluminescence assays were transduced with an SFG vector containing EGFP and firefly luciferase (GFPffLuc) and sorted for GFP-positive cells and maintained in RPMI as above. Human T cells were cultured with RPMI supplemented with 10% FBS and pen/strep and stimulated with IL-2 (Proleukin; Novartis, Basel, Switzerland) every 2–3 days in culture.

CAR T cell production

Human T cells were isolated from buffy coats obtained from the New York Blood Center or from Leukopacks obtained from STEMCELL Technologies (Vancouver, BC, Canada) using a T cell selection kit (Cat# 17951, STEMCELL Technologies, Vancouver, BC, Canada) and transduced with CAR-containing retroviral supernatants as previously described.[41] Briefly, to generate SFG viral producer cell lines, SFG plasmids were either transfected into H29 VSVg viral producing cells (MSK) or co-transfected with pgag/pol (Addgene clone 14887, a gift from Dr. Tannishtha Reya[42]) and VSVg-expressing pMD2.g (Addgene clone 12259, a gift from Dr. Didier Trono) using the ProFection Mammalian Transfection System (Cat# E1200, Promega, Madison, WI). Twenty-four-hour supernatants were collected on days 5 and 6 post-transfection and filtered through 45-μm filters (Cat# 431220, Corning, Glendale, AZ), and used to transduce 293TGalV9 retroviral packaging cells lines (MSK) with the addition of polybrene (Cat# TR-1003-G, Millipore, Burlington, MA) at a final concentration of 8 μg/mL. Viral supernatants from these cells were used for transduction into T cells to generate TA99-CAR T cells. T cells were plated on retronectin-coated plates (Cat# T100B, Takara, Kusatsu, Japan), combined with retroviral supernatants, and spinoculated for 1 h at 2,000 × *g* at room temperature in an Eppendorf (Hamburg, Germany) 5810R centrifuge (rotor A-4-81). Transduction efficiency was assayed using flow cytometry for the FLAG epitope on the CAR for the TA99 CAR and V5 epitope tag for the control CAR constructs, or for the G4S linker in the CAR scFvs.

In vitro cytotoxicity assays

Human CAR T cells were co-cultured with tumor cells over a range of effector (T cell) to tumor cell (E:T) ratios. A total of 5×10^4 tumor cells were plated into black flat-bottom 96-well plates (Cat# 655086, Greiner, Kremsmünster, Austria). Appropriate amounts of CAR T cells were added to achieve the appropriate E:T ratios. All conditions were plated in triplicate, and all constructs were tested using three separate T cell donors (all comparisons use cells from the same donor). Plates were then incubated for 24 h at 37°C in a tissue culture incubator. Five microliters of D-Luciferin (15 mg/mL, Cat# LUCK-1G, Gold Biotechnology, St. Louis, MO) was added to each well of the 96-well plate. Luminescence was measured using a microplate reader (Tecan, Männedorf, Switzerland), and results were exported to Excel (Microsoft, Redmond, WA). For each condition, mean luminescence readings from three wells were averaged and normalized to the average of empty wells, then compared with the average of untreated tumor cells to calculate a percent tumor cell killing value. Negative values (compared with the normalized empty wells) were replaced with zero for analysis. Results were then analyzed and plotted using Prism (GraphPad, San Diego, CA/Boston, MA). Cytotoxicity assays were repeated with human T cells from at least three different donors.

Cytokine measurement

Tumor cells and CAR T cells were co-cultured with tumor cells at equal ratios (1×10^6 cells each) for 24 h. Supernatant from cocultures was collected and assayed using the Milliplex Human Cytokine/chemokine/growth Factor Panel (Cat# HCYTA-60K-PX48, Millipore, Burlington, MA) and assayed on a Luminex Magpix machine using the supplied Xponent software (Luminex, Austin, TX). Kit reagents apart from the standard were diluted 1:5; otherwise, samples were analyzed per the supplier's instructions.

In vivo tumor measurements

All animal studies were conducted in compliance with Memorial Sloan Kettering Institutional Animal Care and Use Committee (IACUC)-approved protocols 00-05-065 and 21-11-008, and Weill Cornell Medicine Institutional Animal Care and Use Committee-approved protocol 2022-0032. Six- to 8-week-old NOD.Cg-Prkdc^{scid} Il2rg^{tm1Wjl}/SzJ (NSG) mice were purchased from the Jackson Laboratory (Bar Harbor, ME). SK-MEL-19 melanoma cells harboring a GFP-firefly luciferase (GFPffLuc) were resuspended in Matrigel (Corning, Corning, NY) and 2×10^6 cells were implanted subcutaneously. After 10 days for engraftment, 5×10^6 human CAR T cells were administered via tail vein injection. Mice were monitored for xenogeneic graft vs. host disease (xGvHD) and other toxicities and were euthanized when they exhibited clinical symptoms of toxicity including lethargy, discomfort, and unkempt coat as per our IACUC-approved protocol. Tumor volumes were assessed weekly using caliper measurements and bioluminescence. For *in vivo*

bioluminescence imaging (BLI), D-luciferin (15 mg/mL, Cat# LUCK-1G, Gold Biotechnology, St. Louis, MO) was administered via retro-orbital injection at a dose of 150 mg/kg in a volume of 100 μL, and bioluminescence signal was measured using an IVIS Spectrum and analyzed using Living Image software (PerkinElmer, Waltham, MA).

Flow cytometry

Anti-TYRP1 antibody (clone TA99) conjugated to Alexa Fluor 647 (Cat# NBP2-34720AF647) and mouse IgG2a Kappa isotype control conjugated to Alexa Fluor 647 (Cat# NBP1-96981AF647) were purchased from Novus Biologicals (Centennial, CO) and used at a concentration of 5 μL per 10^6 cells. Anti-CD19 clone SJ25C1 conjugated to PE (Cat# 12-0198-42) and mouse IgG1 kappa isotype control conjugated to APC (Cat# 17-4714-82) were purchased from eBioscience/Thermo Scientific (Waltham, MA) and used at a concentration of 5 μL per 10^6 cells. Anti-MUC16 antibody 4H11 was obtained from the MSK Bioresource Core Facility[43] (New York, NY) and used at a 1:10,000 dilution using an Alexa 647-labeled goat anti-mouse (VH + VL) antibody (Cat# A21236, Invitrogen) as a secondary stain. Mouse IgG2b (clone E7Q5L) was used as an isotype control (Cat# 53484S, Cell Signaling, Danvers, MA) at a 1:100 dilution and stained with the same Alexa 647 anti-mouse secondary antibody. Anti-FLAG epitope antibody clone L5 conjugated to APC was purchased from BioLegend (San Diego, CA) and used at a 1:10,000 dilution. Anti-V5 tag clone TCM5 conjugated to PE was purchased from eBioscience/Invitrogen (Cat# 12-6796-42, Carlsbad, CA). Anti-G4S-Linker conjugated to Alexa 647 was purchased from Cell Signaling Technology (Cat# 69782S) and used at a 1:400 dilution. DAPI (Cat# D9542, Sigma Aldrich, St. Louis, MO) was used at a 1:1,000 dilution. Cells were analyzed using BD Bioscience LSR Fortessa (BD Bioscience, Franklin Lakes, NJ), Attune (Invitrogen, Waltham, MA), or Cytek Aurora (Freemont, CA) flow cytometers and analyzed using FlowJo (Ashland, OR).

Pathology

Mice were euthanized with CO_2 per IACUC-approved protocol guidelines. Following gross examination, all organs were fixed in 10% neutral buffered formalin, followed by decalcification of bone in a formic acid solution (Surgipath Decalcifier I, Leica Biosystems, Nussloch, Germany). Tissues were then processed in ethanol and xylene and embedded in paraffin in a Leica ASP6025 tissue processor. Paraffin blocks were sectioned at 5 μm, stained with hematoxylin and eosin (H&E), and examined by a board-certified veterinary pathologist (A.P.). The following tissues were processed and examined: subcutaneous tumor (additionally reviewed by an anatomic pathologist [N.P.A.]), heart, thymus, lungs, liver, gallbladder, kidneys, pancreas, stomach, duodenum, jejunum, ileum, cecum, colon, lymph nodes (submandibular, mesenteric), salivary glands, skin (trunk and head), urinary bladder, uterus, cervix, vagina, ovaries, oviducts, adrenal glands, spleen, thyroid gland, esophagus, trachea, spinal cord, vertebrae, sternum, femur, tibia, stifle join, skeletal muscle, nerves, skull, nasal cavity, oral cavity, teeth, ears, eyes, pituitary gland, and brain.

Immunohistochemistry

Immunohistochemistry for TYRP1 was performed on paraffin sections of selected tissues using a Leica Bond RX automated stainer. After heat-induced epitope retrieval in a pH 9.0 buffer, anti-TYRP1 rabbit IgG clone EPR13063 (Cat# ab178676, Abcam, Cambridge, UK), was applied at a concentration of 1:1,000 (0.36 μg/mL), followed by a polymer anti-rabbit IgG detection reagent kit according to the manufacturer's instructions (Cat# DS9800, Novocastra Bond Polymer Refine Detection, Leica Biosystems, Nussloch, Germany). The chromogen indicating positive immunoreactivity was 3,3 diaminobenzidine tetrachloride (DAB), and sections were counterstained with hematoxylin. IHC validation and interpretation were performed by a board-certified veterinary pathologist (S.M.).

DATA AND CODE AVAILABILITY

All source data used in the RNA analysis are available at the references listed in the results and materials and methods sections.

ACKNOWLEDGMENTS

We thank members of the Brentjens and Merghoub/Wolchok labs for technical assistance and support for this work. We thank Dr. Lucia Morgado Palacin for helpful comments on the manuscript. We thank Dr. Frances Weis-Garcia from the MSK Bioresource Core facility for assistance with antibodies and cell lines. C.S.H., T.J.P., S.M., and R.J.B. are supported by NCI grant 1U01CA256801. C.S.H. is additionally supported by NCI grants K12 CA184746 and the NIH SPORE in Soft Tissue Sarcoma P50 CA217694, the Ira Schneider Memorial Cancer Research Foundation and awards from the MSK Technology Development Fund. D.H., M.S.T., Y.M., C.L., J.D.W., and T.M. are supported by NCI grants R01 CA249294–04, R01 CA262516–02, R01 CA286507-01, UE5 CA246754, U01 CA271407, and U10 CA180820, the WCM Prostate Cancer SPORE P50 CA211024, DOD grants W81XWH-20-1-0723 and W81XWH-21-1-0101, The Breast Cancer Research Foundation, the Mark Foundation, the Parker Institute for Cancer Immunotherapy, Ludwig Institute for Cancer Research, Swim Across America, the Melanoma Research Alliance, and Stand Up To Cancer. This work was additionally supported by the MSK NCI Comprehensive Cancer Center Support Grant P30 CA008748.

AUTHOR CONTRIBUTIONS

C.S.H. and D.H. conceptualized the work, planned and performed experiments, and analyzed data. M.S.T., T.J.P., C.L., and S.E.S. performed experiments and analyzed data. Y.M. performed bioinformatics data analysis. A.P., N.P.A., and S.M. conceptualized work and performed expert data analysis. E.d.S. coordinated work, curated data, and provided resources. S.R. conceptualized work, provided methodology, and planned experiments. C.S.H., J.D.W., T.M., and R.J.B. acquired the funding and coordinated the project. C.S.H. drafted the manuscript under the direction of J.D.W., T.M., and R.J.B. and with the assistance of all other authors. J.D.W., T.M., and R.J.B. supervised the work.

DECLARATION OF INTERESTS

C.S.H., D.H., T.J.P., S.R., J.D.W., T.M., and R.J.B. are inventors on multiple patents filed by MSK covering CAR T cell technology, including the CAR T cells discussed in this manuscript. S.R. serves on the Scientific Advisory Board of Celyad Oncology. R.J.B. has licensed intellectual property to and collects royalties from BMS, Caribou, and Sanofi. R.J.B. received research funding from BMS. R.J.B. is a consultant to BMS, Atara Biotherapeutics Inc., and Triumvira, and was a consultant for Cargo Tx and CoImmune but ended in the past 3 months, and Gracell Biotechnologies Inc. but ended employment in the past 24 months. R.J.B. is a member of the scientific advisory board for Triumvira and was a member of the scientific advisory board for Cargo Tx and CoImmune, but that ended in the past 6 months. J.D.W. is a consultant for Apricity, Ascentage Pharma, AstraZeneca, BeiGene, Bicara Therapeutics (ending 4/1/2024), Bristol Myers Squibb, Daiichi Sankyo, Dragonfly, Imvaq, Larkspur, Psioxus, Recepta, Takeda, Tizona, Trishula Therapeutics, and Sellas. J.D.W. received grant/research support from Bristol Myers Squibb and Enterome. J.D.W. has equity in Apricity, Arsenal IO/CellCarta, Ascentage, Imvaq, Linneaus, Larkspur, Georgiamune, Maverick, Tizona Therapeutics, and Xenimmune. J.D.W. is an inventor on the following patents: Xenogeneic DNA Vaccines, Newcastle Disease viruses for Cancer Therapy, Myeloid-derived suppressor cell (MDSC)

assay, Prediction of responsiveness to treatment with immunomodulatory therapeutics and method of monitoring abscopal effects during such treatment, Anti-PD1 Antibody, Anti-CTLA4 antibodies, Anti-GITR antibodies and methods of use thereof. T.M. is a consultant for Immunos Therapeutics, Daiichi Sankyo Co, TigaTX, Normunity, and Pfizer. T.M. is a cofounder of and equity holder in Imvaq Therapeutics. T.M. receives research grant funding from Bristol Myers Squibb, Surface Oncology, Kyn Therapeutics, Infinity Pharmaceuticals, Peregrine Pharmaceuticals, Adaptive Biotechnologies, Leap Therapeutics, and Aprea Therapeutics. T.M. is an inventor on patent applications related to work on oncolytic viral therapy, alpha virus-based vaccine, *neo*-antigen modeling, CD40, GITR, OX40, PD-1, and CTLA-4.

SUPPLEMENTAL INFORMATION

Supplemental information can be found online at https://doi.org/10.1016/j.omton.2024.200862.

REFERENCES

1. Wolchok, J.D., Chiarion-Sileni, V., Gonzalez, R., Rutkowski, P., Grob, J.J., Cowey, C.L., Lao, C.D., Wagstaff, J., Schadendorf, D., Ferrucci, P.F., et al. (2017). Overall Survival with Combined Nivolumab and Ipilimumab in Advanced Melanoma. N. Engl. J. Med. *377*, 1345–1356. https://doi.org/10.1056/NEJMoa1709684.
2. Sarnaik, A.A., Hamid, O., Khushalani, N.I., Lewis, K.D., Medina, T., Kluger, H.M., Thomas, S.S., Domingo-Musibay, E., Pavlick, A.C., Whitman, E.D., et al. (2021). Lifileucel, a Tumor-Infiltrating Lymphocyte Therapy, in Metastatic Melanoma. J. Clin. Oncol. *39*, 2656–2666. https://doi.org/10.1200/JCO.21.00612.
3. Goff, S.L., Dudley, M.E., Citrin, D.E., Somerville, R.P., Wunderlich, J.R., Danforth, D.N., Zlott, D.A., Yang, J.C., Sherry, R.M., Kammula, U.S., et al. (2016). Randomized, Prospective Evaluation Comparing Intensity of Lymphodepletion Before Adoptive Transfer of Tumor-Infiltrating Lymphocytes for Patients With Metastatic Melanoma. J. Clin. Oncol. *34*, 2389–2397. https://doi.org/10.1200/Jco.2016.66.7220.
4. Curti, B.D., and Faries, M.B. (2021). Recent Advances in the Treatment of Melanoma. N. Engl. J. Med. *384*, 2229–2240. https://doi.org/10.1056/NEJMra2034861.
5. Hassel, J.C., Piperno-Neumann, S., Rutkowski, P., Baurain, J.F., Schlaak, M., Butler, M.O., Sullivan, R.J., Dummer, R., Kirkwood, J.M., Orloff, M., et al. (2023). Three-Year Overall Survival with Tebentafusp in Metastatic Uveal Melanoma. N. Engl. J. Med. *389*, 2256–2266. https://doi.org/10.1056/NEJMoa2304753.
6. Siegel, R.L., Miller, K.D., and Jemal, A. (2019). Cancer statistics, 2019. CA A Cancer J. Clin. *69*, 7–34. https://doi.org/10.3322/caac.21551.
7. Zaretsky, J.M., Garcia-Diaz, A., Shin, D.S., Escuin-Ordinas, H., Hugo, W., Hu-Lieskovan, S., Torrejon, D.Y., Abril-Rodriguez, G., Sandoval, S., Barthly, L., et al. (2016). Mutations Associated with Acquired Resistance to PD-1 Blockade in Melanoma. N. Engl. J. Med. *375*, 819–829. https://doi.org/10.1056/NEJMoa1604958.
8. Lee, J.H., Shklovskaya, E., Lim, S.Y., Carlino, M.S., Menzies, A.M., Stewart, A., Pedersen, B., Irvine, M., Alavi, S., Yang, J.Y.H., et al. (2020). Transcriptional downregulation of MHC class I and melanoma de- differentiation in resistance to PD-1 inhibition. Nat. Commun. *11*, 1897. https://doi.org/10.1038/s41467-020-15726-7.
9. Rafiq, S., Hackett, C.S., and Brentjens, R.J. (2020). Engineering strategies to overcome the current roadblocks in CAR T cell therapy. Nat. Rev. Clin. Oncol. *17*, 147–167. https://doi.org/10.1038/s41571-019-0297-y.
10. Sadelain, M., Rivière, I., and Riddell, S. (2017). Therapeutic T cell engineering. Nature *545*, 423–431. https://doi.org/10.1038/nature22395.
11. Vijayasaradhi, S., Bouchard, B., and Houghton, A.N. (1990). The Melanoma Antigen Gp75 Is the Human Homolog of the Mouse-B (Brown) Locus Gene-Product. J. Exp. Med. *171*, 1375–1380. https://doi.org/10.1084/jem.171.4.1375.
12. Thomson, T.M., Real, F.X., Murakami, S., Cordoncardo, C., Old, L.J., and Houghton, A.N. (1988). Differentiation Antigens of Melanocytes and Melanoma - Analysis of Melanosome and Cell-Surface Markers of Human Pigmented Cells with Monoclonal-Antibodies. J. Invest. Dermatol. *90*, 459–466. https://doi.org/10.1111/1523-1747.ep12460906.
13. Thomson, T.M., Mattes, M.J., Roux, L., Old, L.J., and Lloyd, K.O. (1985). Pigmentation-Associated Glycoprotein of Human Melanomas and Melanocytes - Definition with a Mouse Monoclonal-Antibody. J. Invest. Dermatol. *85*, 169–174. https://doi.org/10.1111/1523-1747.ep12276608.
14. Naftzger, C., Takechi, Y., Kohda, H., Hara, I., Vijayasaradhi, S., and Houghton, A.N. (1996). Immune response to a differentiation antigen induced by altered antigen: a study of tumor rejection and autoimmunity. Proc. Natl. Acad. Sci. USA *93*, 14809–14814. https://doi.org/10.1073/pnas.93.25.14809.
15. Khalil, D.N., Postow, M.A., Ibrahim, N., Ludwig, D.L., Cosaert, J., Kambhampati, S.R.P., Tang, S., Grebennik, D., Kauh, J.S.W., Lenz, H.J., et al. (2016). An Open-Label, Dose-Escalation Phase I Study of Anti-TYRP1 Monoclonal Antibody IMC-20D7S for Patients with Relapsed or Refractory Melanoma. Clin. Cancer Res. *22*, 5204–5210. https://doi.org/10.1158/1078-0432.CCR-16-1241.
16. Ma, L., Dichwalkar, T., Chang, J.Y.H., Cossette, B., Garafola, D., Zhang, A.Q., Fichter, M., Wang, C., Liang, S., Silva, M., et al. (2019). Enhanced CAR-T cell activity against solid tumors by vaccine boosting through the chimeric receptor. Science *365*, 162–168. https://doi.org/10.1126/science.aav8692.
17. Ma, L., Hostetler, A., Morgan, D.M., Maiorino, L., Sulkaj, I., Whittaker, C.A., Neeser, A., Pires, I.S., Yousefpour, P., Gregory, J., et al. (2023). Vaccine-boosted CAR T crosstalk with host immunity to reject tumors with antigen heterogeneity. Cell *186*, 3148–3165.e20. https://doi.org/10.1016/j.cell.2023.06.002.
18. Brog, R.A., Ferry, S.L., Schiebout, C.T., Messier, C.M., Cook, W.J., Abdullah, L., Zou, J., Kumar, P., Sentman, C.L., Frost, H.R., and Huang, Y.H. (2022). Superkine IL-2 and IL-33 Armored CAR T Cells Reshape the Tumor Microenvironment and Reduce Growth of Multiple Solid Tumors. Cancer Immunol. Res. *10*, 962–977. https://doi.org/10.1158/2326-6066.CIR-21-0536.
19. Zhao, Y., Chen, J., Andreatta, M., Feng, B., Xie, Y.Q., Wenes, M., Wang, Y., Gao, M., Hu, X., Romero, P., et al. (2024). IL-10-expressing CAR T cells resist dysfunction and mediate durable clearance of solid tumors and metastases. Nat. Biotechnol. https://doi.org/10.1038/s41587-023-02060-8.
20. Jilani, S., Saco, J.D., Mugarza, E., Pujol-Morcillo, A., Chokry, J., Ng, C., Abril-Rodriguez, G., Berger-Manerio, D., Pant, A., Hu, J., et al. (2024). CAR-T cell therapy targeting surface expression of TYRP1 to treat cutaneous and rare melanoma subtypes. Nat. Commun. *15*, 1244. https://doi.org/10.1038/s41467-024-45221-2.
21. Muranski, P., Boni, A., Antony, P.A., Cassard, L., Irvine, K.R., Kaiser, A., Paulos, C.M., Palmer, D.C., Touloukian, C.E., Ptak, K., et al. (2008). Tumor-specific Th17-polarized cells eradicate large established melanoma. Blood *112*, 362–373. https://doi.org/10.1182/blood-2007-11-120998.
22. Cancer Genome Atlas Research Network, Weinstein, J.N., Collisson, E.A., Mills, G.B., Shaw, K.R.M., Ozenberger, B.A., Ellrott, K., Shmulevich, I., Sander, C., and Stuart, J.M. (2013). The Cancer Genome Atlas Pan-Cancer analysis project. Nat. Genet. *45*, 1113–1120. https://doi.org/10.1038/ng.2764.
23. Zhang, C., Shen, H., Yang, T., Li, T., Liu, X., Wang, J., Liao, Z., Wei, J., Lu, J., Liu, H., et al. (2022). A single-cell analysis reveals tumor heterogeneity and immune environment of acral melanoma. Nat. Commun. *13*, 7250. https://doi.org/10.1038/s41467-022-34877-3.
24. Ghandi, M., Huang, F.W., Jané-Valbuena, J., Kryukov, G.V., Lo, C.C., McDonald, E.R., 3rd, Barretina, J., Gelfand, E.T., Bielski, C.M., Li, H., et al. (2019). Next-generation characterization of the Cancer Cell Line Encyclopedia. Nature *569*, 503–508. https://doi.org/10.1038/s41586-019-1186-3.
25. GTEx Consortium (2013). The Genotype-Tissue Expression (GTEx) project. Nat. Genet. *45*, 580–585. https://doi.org/10.1038/ng.2653.
26. Chekmasova, A.A., Rao, T.D., Nikhamin, Y., Park, K.J., Levine, D.A., Spriggs, D.R., and Brentjens, R.J. (2010). Successful eradication of established peritoneal ovarian tumors in SCID-Beige mice following adoptive transfer of T cells genetically targeted to the MUC16 antigen. Clin. Cancer Res. *16*, 3594–3606. https://doi.org/10.1158/1078-0432.CCR-10-0192.
27. Brentjens, R.J., Davila, M.L., Riviere, I., Park, J., Wang, X., Cowell, L.G., Bartido, S., Stefanski, J., Taylor, C., Olszewska, M., et al. (2013). CD19-targeted T cells rapidly induce molecular remissions in adults with chemotherapy-refractory acute lymphoblastic leukemia. Sci. Transl. Med. *5*, 177ra38. https://doi.org/10.1126/scitranslmed.3005930.
28. du Rusquec, P., de Calbiac, O., Robert, M., Campone, M., and Frenel, J.S. (2019). Clinical utility of pembrolizumab in the management of advanced solid tumors: an evidence-based review on the emerging new data. Cancer Manag. Res. *11*, 4297–4312. https://doi.org/10.2147/CMAR.S151023.

29. Wong, A.C.Y., and Ma, B. (2016). An update on the pharmacodynamics, pharmacokinetics, safety and clinical efficacy of nivolumab in the treatment of solid cancers. Expet Opin. Drug Metabol. Toxicol. *12*, 1255–1261. https://doi.org/10.1080/17425255.2016.1223047.

30. Atkins, M.B., Curiel-Lewandrowski, C., Fisher, D.E., Swetter, S.M., Tsao, H., Aguirre-Ghiso, J.A., Soengas, M.S., Weeraratna, A.T., Flaherty, K.T., Herlyn, M., et al. (2021). The State of Melanoma: Emergent Challenges and Opportunities. Clin. Cancer Res. *27*, 2678–2697. https://doi.org/10.1158/1078-0432.CCR-20-4092.

31. Thistlethwaite, F.C., Gilham, D.E., Guest, R.D., Rothwell, D.G., Pillai, M., Burt, D.J., Byatte, A.J., Kirillova, N., Valle, J.W., Sharma, S.K., et al. (2017). The clinical efficacy of first-generation carcinoembryonic antigen (CEACAM5)-specific CAR T cells is limited by poor persistence and transient pre-conditioning-dependent respiratory toxicity. Cancer Immunol. Immunother. *66*, 1425–1436. https://doi.org/10.1007/s00262-017-2034-7.

32. Lamers, C.H., Sleijfer, S., van Steenbergen, S., van Elzakker, P., van Krimpen, B., Groot, C., Vulto, A., den Bakker, M., Oosterwijk, E., Debets, R., and Gratama, J.W. (2013). Treatment of metastatic renal cell carcinoma with CAIX CAR-engineered T cells: clinical evaluation and management of on-target toxicity. Mol. Ther. *21*, 904–912. https://doi.org/10.1038/mt.2013.17.

33. Chandran, S.S., and Klebanoff, C.A. (2019). T cell receptor-based cancer immunotherapy: Emerging efficacy and pathways of resistance. Immunol. Rev. *290*, 127–147. https://doi.org/10.1111/imr.12772.

34. Xu, Y., Setaluri, V., Takechi, Y., and Houghton, A.N. (1997). Sorting and secretion of a melanosome membrane protein, gp75/TRP1. J. Invest. Dermatol. *109*, 788–795. https://doi.org/10.1111/1523-1747.ep12340971.

35. Bluhm, J., Kieback, E., Marino, S.F., Oden, F., Westermann, J., Chmielewski, M., Abken, H., Uckert, W., Höpken, U.E., and Rehm, A. (2018). CAR T Cells with Enhanced Sensitivity to B Cell Maturation Antigen for the Targeting of B Cell Non-Hodgkin's Lymphoma and Multiple Myeloma. Mol. Ther. *26*, 1906–1920. https://doi.org/10.1016/j.ymthe.2018.06.012.

36. Harris, D.T., Hager, M.V., Smith, S.N., Cai, Q., Stone, J.D., Kruger, P., Lever, M., Dushek, O., Schmitt, T.M., Greenberg, P.D., and Kranz, D.M. (2018). Comparison of T Cell Activities Mediated by Human TCRs and CARs That Use the Same Recognition Domains. J. Immunol. *200*, 1088–1100. https://doi.org/10.4049/jimmunol.1700236.

37. Liu, Y., Liu, G., Wang, J., Zheng, Z.Y., Jia, L., Rui, W., Huang, D., Zhou, Z.X., Zhou, L., Wu, X., et al. (2021). Chimeric STAR receptors using TCR machinery mediate robust responses against solid tumors. Sci. Transl. Med. *13*, eabb5191. https://doi.org/10.1126/scitranslmed.abb5191.

38. Li, B., Ruotti, V., Stewart, R.M., Thomson, J.A., and Dewey, C.N. (2010). RNA-Seq gene expression estimation with read mapping uncertainty. Bioinformatics *26*, 493–500. https://doi.org/10.1093/bioinformatics/btp692.

39. Wickham, H. (2016). ggplot2 : Elegant Graphics for Data Analysis. Use R!, 2nd ed. (Springer International Publishing: Imprint: Springer).

40. Riviere, I., Brose, K., and Mulligan, R.C. (1995). Effects of retroviral vector design on expression of human adenosine deaminase in murine bone marrow transplant recipients engrafted with genetically modified cells. Proc. Natl. Acad. Sci. USA *92*, 6733–6737. https://doi.org/10.1073/pnas.92.15.6733.

41. Rafiq, S., Yeku, O.O., Jackson, H.J., Purdon, T.J., van Leeuwen, D.G., Drakes, D.J., Song, M., Miele, M.M., Li, Z., Wang, P., et al. (2018). Targeted delivery of a PD-1-blocking scFv by CAR-T cells enhances anti-tumor efficacy in vivo. Nat. Biotechnol. *36*, 847–856. https://doi.org/10.1038/nbt.4195.

42. Reya, T., Duncan, A.W., Ailles, L., Domen, J., Scherer, D.C., Willert, K., Hintz, L., Nusse, R., and Weissman, I.L. (2003). A role for Wnt signalling in self-renewal of haematopoietic stem cells. Nature *423*, 409–414. https://doi.org/10.1038/nature01593.

43. Dharma Rao, T., Park, K.J., Smith-Jones, P., Iasonos, A., Linkov, I., Soslow, R.A., and Spriggs, D.R. (2010). Novel monoclonal antibodies against the proximal (carboxy-terminal) portions of MUC16. Appl. Immunohistochem. Mol. Morphol. *18*, 462–472. https://doi.org/10.1097/PAI.0b013e3181dbfcd2.